International Journal of ChemTech Research
CODEN (USA): IJCRGG ISSN: 0974-4290
Vol.8, No.8, pp 333-348, 2015

Catalytic Pyrolysis of Plastic Waste into Activated Carbon and its Adsorption Studies on Acid Red 114 as Model Organic Pollutant

T.K.Manimekalai[1], N.Sivakumar[2]* & S.Periyasamy[3]

[1]Department of Chemistry, J. K. K. Munirajah College of Technology, T.N.Palayam, Gobi, Erode-638506, India
[2]Department of Chemistry, Chikkanna Government Arts and Science College, Tirupur-641602, India
[3]Department of Textile Technology, PSG College of Technology, Coimbatore-641004, India

Abstract: Plastic waste activated through CO_2 carbon (PWAC) was studied as an adsorbent for the removal of acid red 114 from textile industry effluent. Plastic waste carbon was obtained from pyrolysis of commonly used three polymer materials PP, PVC and PET at 600 °C in N_2 atmosphere. AC activated carbon was analyzed by SEM, FTIR and EDAX. The adsorption capacity of the acid red 114 dye was evaluated through equilibrium and kinetic studies. Equilibrium isotherms were analyzed by Langmuir, Freundlich, Dubinin–Radushkevich, Temkin, Jovanovic and Halsey models. Langmuir isotherm model showed a best fit for the adsorption of acid red 114 with maximum monolayer coverage of 159.18 mg/g. The adsorption capacity of AC was strongly dependent on the temperature and external surface of the activated carbon. The experimental data were applied to adsorption kinetic models and the results indicated that the adsorption behavior of PWAC was described very well by the second-order kinetics model with high correlation coefficients. The thermodynamic parameters (ΔH^o, ΔS^o, and ΔG^o) showed that the adsorption of acid red 114 was feasible, exothermic and spontaneous at 303, 318 and 333 K.
Keywords: Plastic waste activated carbon; Adsorption; Isotherm model; Acid red ; Thermodynamics; Kinetics; Error analysis.

1. Introduction

A polymeric material, the plastic has become the integral part of everybody in the present world. It has replaced many engineering structural materials. It is used from lower end like polyethylene bags to higher end applications like spacecrafts. It is being used in large quantities and growth rate is increasing every year to meet various consumer demands and technology development. Through the polymer serves such applications with techno-economical benefits, the challenge which remains is the disposal. The usage and disposal are diverse and include accumulation of plastics waste in landfills generating a major health and environmental problem all over the world [1]. The most usual ways of dealing with these wastes are incineration, energy recovery and mechanical recycling. The conversion of plastics waste into value added products is another way to overcome the above problems. The pyrolysis, gasification and hydrogenation are environmentally and economically enhancing method for plastic wastes consumption [2]. Catalytic pyrolysis of plastic waste conversion is a

superior method of reusing the waste [3]. As catalyst play an important role, many researchers have worked on various catalysts and their combinations for pyrolysis studies of polymeric materials [4-6]. In this study, pyrolysis of Polyvinyl chloride (PVC), Polyethyleneterepthalate (PET) and Polypropylene (PP) with HZSM -5 catalyst have been studied and reported. It has been revealed that the proposed method would allow for modifying the catalytic pyrolysis process of the selected polymer to produce high market value hydrocarbons with low energy consumption [7-8]. The solid residual char obtained from the pyrolysis process is a carbon-rich adsorbent material that can be used as carbon black or, otherwise, upgraded to activated carbon [9]. Adsorption is one of the best process has been used for wastewater purification technique for the removal of organic molecules at industrial scale [10]. Activated carbons having mesoporous–microporous structure are widely used as adsorbents for the removal of organic pollutants from textile industrial effluents or wastewaters [11-12]. Hence the char obtained in the proposed pyrolysis process has been used for dye adsorption studies. Thus the work essentially reports on characterization of PWAC, removal of the model organic pollutant i.e. acid red 114 from textile industrial effluents, thermodynamic studies of acid red 114 adsorption and finally the mechanism determining the observed efficiency of PWAC.

2. Materials and Methods

2.1. Materials

The waste plastics was collected from kitchen appliances, containers, kettles, straws and syringes was made by PP. Drinking bottles and flexible food packages, space blankets and medicine jars was made by PET. Pipes, roof sheeting, cosmetic containers, window and floor frames and blood bags was made by PVC. HZSM-5 catalyst was obtained from a Sud-Chemie India Pvt. Ltd.

2.2. Preparation of PWAC

The plastic mixture used for the experiment comprises 38% polyethyleneterepthalate (PET), 38% polyvinyl chloride (PVC) and 19% polypropylene (PP) along with 5% HZSM-5 were placed in tubular reactor and heated to 600 °C at 10 °C min^{-1} and kept for 1h in N_2 atmosphere. 10% carbon yield was obtained after the pyrolysis and residues were powdered with mortar and then washed with 200 ml of concentrated hydrochloric acid using magnetic stirrer for 1h to remove the inorganic impurities. Finally the residue was rinsed with distilled water until the filtrate's p^H becomes 7. The final char was dried in a hot air oven at 100 °C and it was left to cool over-night. The final activation of the char was carried out in a specially designed stainless steel reactor at 900 °C in the presence of CO_2.

2.3. Preparation of adsorbate

Acid red 114 (CI= 23635, chemical formula $C_{37}H_{28}N_4Na_2O_{10}S_3$, MW= 830.81g/mol) dye was obtained from a textile dying factory unit ($\lambda_{max\ (abs)}$-514 nm). Precise quantities of solid dye were dissolved in double distilled water to prepare the stock solutions of Acid red 114 Solutions of various concentrations of dye were obtained by diluting this stock solution. The pH of the prepared solutions was adjusted by using HCl and NaOH solutions of strength 0.01N.

2.4 Characterization of PWAC

The Morphological characteristics of the sample was studied using JSM-5610LV Scanning Electron Microscope (SEM).X-ray diffraction spectroscopy (XRD) analyses was carried out with PANalytical X-ray instrument. The N_2 adsorption-desorption isotherms of activated carbon was measured at 77K using N_2 adsorption analyser (Nova, Quantachrome instrument). Fourier Transform Infrared (FT-IR) measurements were carried out using Shimadzu instrument.

2.5 Adsorption Experiments

2.5.1 Isotherm Model

As a suitable measure for determination of the relationship between self-governing and dependent variables, the coefficient of determination was used in this study. To estimate the best apt of the isotherm models to the experimental data, the optimization technique require different statistical parameters to be well-defined. In our study, the best fit model was appraised by the Sum of the Square of the Errors (SSE), the Residual Root Mean Square Error (RMSE) and the chi-square test χ^2 expressed as follows [13-14]

$$SSE = \sum (q_{e,cal} - q_{e,exp})^2$$

$$RMSE = \sum \frac{1}{N-2} \sum_{i=1}^{n} (q_{e,exp} - q_{e,cal})^2$$

$$\chi^2 = \sum_{i=1}^{n} \frac{(q_{e,exp} - q_{e,cal})^2}{q_{e,exp}}$$

Where, n denotes the number of experimental data, $q_{e,cal}$ is calculated equilibrium solid phase concentration, $q_{e,exp}$ is measured equilibrium solid phase concentration. The advantage of using the chi-square test was the comparison of all isotherms on the same abscissa and ordinate. If data from the model were similar to the experimental data, χ^2 would be a small number or vice versa.

3. Results and discussion

3.1. Scanning Electron Microscope analysis

The SEM images of activated carbon are given in Fig. 1a, Fig. 1b & Fig. 1c. It can be seen that the PWAC is consists of agglomerates of carbon black structures. Large amount of mesopores and macropores are formed, it was shown in Fig. 1a. The inner carbonaceous phase also becomes fragmented, indicating that the carbon skeleton is severely broken and a "loose sponge" structure is formed during the activating process. The surface of PWAC looks much smoother and pores are arranged irregularly. Small pores can be seen on the inner walls of larger pores. Making it difficult to determine individual particle size by SEM analysis [15].

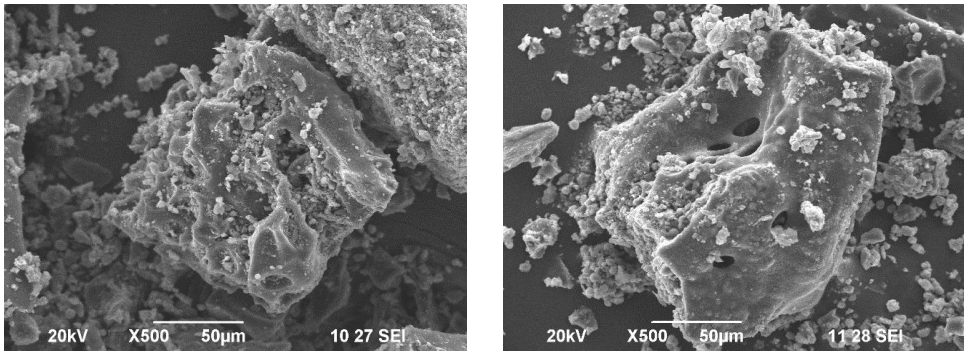

(a) **(b)**

Fig. 1 Scanning electron micrograph of a) pyrolysed char and b) PWAC

3.2. XRD Analysis of PWAC

The X-ray pattern can be used to confirm that the sample being analyzed is amorphous or crystalline. Amorphous materials do not have long range order like crystalline materials and therefore the resulting diffraction pattern show the typical series of peaks associated with crystalline materials. The diffraction pattern of materials shows a broad "halo" with few or single maxima, Fig. 2. Although this "halo" pattern uniquely identify the material being studied it confirm that the material is crystalline, which is critical knowledge needed for characterization. While, powder X-ray diffraction is used to identify and monitor the crystalline solid form of the active ingredient in a small molecule formulation of excipient form an amorphous or crystalline matrix [16].

The literature of carbon materials repeatedly refers to the crystallite and to the crystallite size, with its graphitic connotations, in analyses of structure within activated carbon based on XRD data. The XRD diagrams of activated carbon prepared from polymeric waste indicate the intense main peak shows the presence of highly organized crystalline structure of activated carbon. This crystalline structure increases the adsorption of dyes onto prepared activated carbon, where the dyes adsorbed on the upper layer of the crystalline structure of the carbon surface by means of physisorption [17].

The strong diffraction peak emerged at $2\theta = 22.97°$ correspond plane indicates the existence of graphite crystallite in plastic waste active carbon [18]. It is generally expected that increasing the pre-carbonization temperature promotes the growth of the graphitic micro-crystallites and sharpens at XRD peaks of the

produced activated carbon [19].The diffraction peak at 2θ = 7.72° correspond plane indicates HZSM-5 catalyst structure [20].

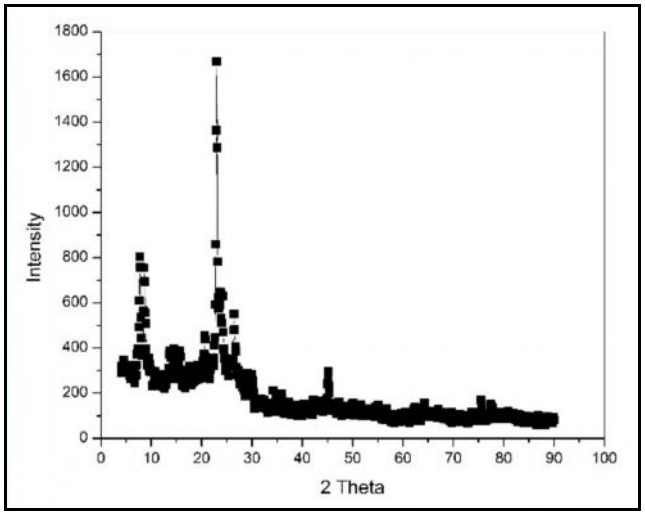

Fig. 2. XRD pattern of PWAC

3.3. Adsorption Isotherm Studies

The simplest method for determination of the isotherm constants for two parameter isotherms is to linearize the model equation and then apply linear regression. The equilibrium measurements were focused on the determination of the adsorption isotherms. The amount of adsorbed dye per unit mass of the plastic waste adsorbent (q_e) and the equilibrium solution dye concentration (C_e) for the temperature range of 30, 45 and 60 °C. It was found that the adsorption capacity increased as the temperature was increased from 30, 45 and 60 °C.

Isotherm data should be accurately fit to a suitable isotherm model to find adsorption parameters that can be used in a single batch design process [21]. There are several isotherm equations available for analyzing experimental sorption equilibrium data in single-solute systems. The most commonly used are the Langmuir, Freundlich, Temkin, D-R, Halsey and Jovanovic models.

3.3.1. Langmuir isotherm

The Langmuir adsorption isotherm is based on the assumption that all sites possess equal affinity for the adsorbate. It may be represented in the linear form as follows [22].

$$\frac{C_e}{q_e} = \frac{1}{K_L Q_m} + \frac{C_e}{Q_m}$$

Where Q_m is the maximum acid red 114 uptake, mg/g, K_L the Langmuir adsorption constant, L/mg. The model provides the maximum values where they could not be reached in the experiments. The values of K_L were decreased with increasing temperature of the studied system. The K_L values indicate adsorption affinity. The monolayer saturation capacity, Q_m, were 105.62, 127.84 and 135.79 mg/L for PWAC at different temperature respectively. From Table 1&2 it can be observed that the calculated isotherm parameters and their corresponding RMSE, SSE and χ^2 values vary for the six linearized types of isotherm models. It can be seen that the Langmuir model yields a better fit than the Freundlich, Temkin model and other isotherm models, as reflected by a RMSE, and χ^2 values. Langmuir isotherm showed better fit followed by Temkin isotherm model in terms of coefficient determination values.

The essential feature of the Langmuir isotherm can be expressed by means of R_L (R_L=1/1+bC_0), a dimensionless constant referred to as separation factor or equilibrium parameter.

Table 1 List of different model isotherm parameter values for acid red 114

Model	Isotherm Constants	Temperature		
		30 °C	**45 °C**	**60 °C**
Langmuir	Q_m(mg g^{-1})	105.62	127.84	135.79
	K_L(L mg^{-1})	0.1120	0.0377	0.0197
	R^2	0.9963	0.9926	0.9928
Freundlich	1/n	0.4902	0.6602	0.7353
	K_f(mg g^{-1})(L mg^{-1})$^{1/n}$	15.2059	6.9103	3.8990
	R^2	0.9719	0.9807	0.9865
Temkin	β_T(KJ mol^{-1})	20.1331	24.8792	24.1672
	b	127.1890	106.2676	112.8388
	α_T(L mg^{-1})	1.6334	0.5066	0.3014
	R^2	0.9745	0.9596	0.9567
Halsey	K_h(mg g^{-1})	257.8739	18.6857	6.3632
	n	2.0401	1.5146	1.3600
	R^2	0.9719	0.9807	0.9865
D-R	K_{DR}(mol^2 KJ^{-2})	5.778E-06	2.906E-05	6.895E-05
	Q_D(mg g^{-1})	61.08	56.96	50.31
	R^2	0.6511	0.6681	0.6807
	E	0.0012	0.0027	0.0042
Jovanovic	q_{max}	1.0433	1.0554	1.0689
	K_J	0.0281	0.0303	0.0274
	R^2	0.5999	0.6937	0.7478

The value of R_L indicated the type of isotherm to be irreversible (R_L=0), favourable (0<R_L<1), linear (R_L=1) or unfavourable (R_L>1). Further, the R_L value for acid red 114 onto PWAC at 30 to 60°C are 0.0598 to 0.746 indicates adsorption process is favourable [23].

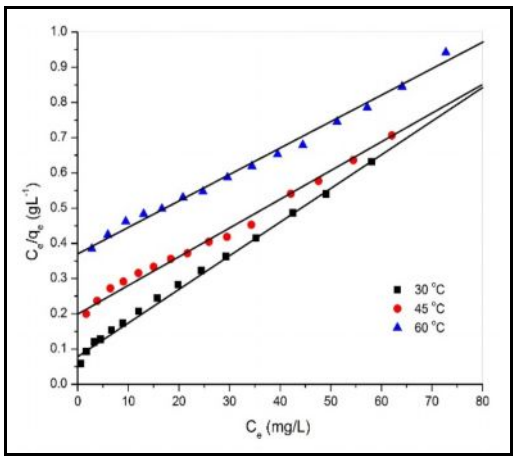

Fig. 3. Effect of Langmuir plot for the adsorption of Acid Red 114 onto PWAC.

3.3.2. Freundlich isotherm

The empirical Freundlich isotherm is based on the equilibrium relationship between heterogeneous surfaces. This isotherm is derived from the assumption that the adsorption sites are distributed exponentially with respect to the heat of adsorption. The logarithmic linear form of Freundlich isotherm may be represented as follows [24].

$$\log q_e = \log K_F + \frac{1}{n}\log C_e$$

These slope values indicated that adsorption intensity n and the intercept values gave an idea about adsorption capacity K_F. Where K_F(L/g) and 1/n are the Freundlich constants, indicating the sorption capacity and sorption intensity, respectively. The magnitude of K_F value decreased with increasing temperature,

indicating that the adsorption process is exothermic in nature. The Freundlich adsorption isotherm was showed in Fig.4.

The 1/n is a measure of adsorption intensity, also indicated that $0 < 1/n < 1$, indicating that acid red 114 is favourably adsorbed by PWAC at all studied parameters. It was learnt that, If n = 1 then that the partition between the two phases was independent of the concentration. If the 1/n value is below one it indicates a normal adsorption. On the other hand 1/n being above one indicates cooperative adsorption [25]. The value of n greater than one confirmed that the activated carbon underwent a favorable for Freundlich isotherm.

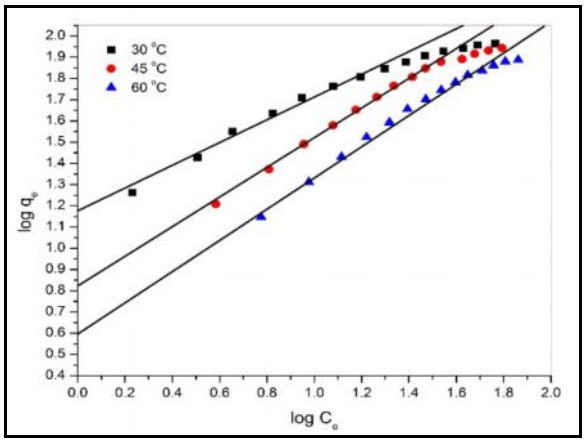

Fig.4. Effect of Freundlich plot for the adsorption of Acid Red 114 onto PWAC.

3.3.3. Temkin isotherm

Temkin isotherm, assumes that the heat of adsorption decreases linearly with the coverage due to adsorbent-adsorbate interaction. The Tempkin isotherm has generally been applied in the following linear form [26].

$$q_e = B\ln A + B\ln C_e$$

Where B=RT/b constant related to heat of sorption. A(L/g) is Temkin isotherm constant, b (J/mol) is a constant related to heat of sorption, R is the gas constant (8.314 J/mol K) and T the absolute temperature (K). A plot of q_e versus $\ln C_e$(Fig.5) enables the determination of the isotherm constants A, b from the slope and intercept.

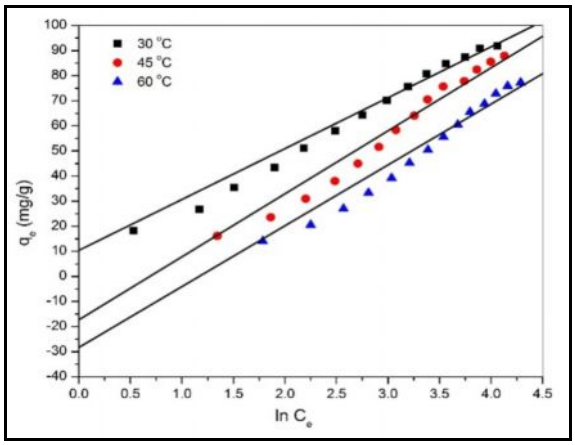

Fig. 5. Effect of Temkin plot for the adsorption of Acid Red 114 onto PWAC.

The heat of dye adsorption (b) is directly related to coverage of dye onto PWAC due to adsorbent-adsorbate interaction. It was decreased with increasing temperature from 127 to 106 J/mol, as listed in Table 1. This indicates that the heat of adsorption of acid red 114 onto the surface of PWAC decreases with increasing temperature from 303 to 333 K and the sorption is exothermic.

3.3.4. Dubinin-Raduchkevich

Dubinin-Raduchkevich are used for estimating the mechanism of surface adsorption. Dubinin and Raduchkevich in 1947 proposed that the adsorption curve depends on the structure of the adsorbent pores [27]. The plot of $\ln q_e$ vs. ε^2 at for acid red 114 is presented in Fig. 6. The constant obtained for D–R isotherms are shown in Table 1. The mean adsorption energy (E) gives information about the chemical and physical nature of adsorption [28].

The linear form of the isotherm can be expressed as follows:

$$\ln q_e = \ln Q_D - B_D \varepsilon^2$$

Where Q_D is the theoretical maximum capacity (mol/g), B_D is the D-R model constant (mol^2/kJ^2), ε is the Polanyi potential and is equal to

$$\varepsilon = RT\ln\left(1 + \frac{1}{C_e}\right)$$

The mean energy of sorption, E(kJ/mol), is calculated by the following equation

$$E = \frac{1}{\sqrt{2B_D}}$$

The Dubinin-Radushkevich, (DR) isotherm model is more general than the Langmuir isotherm as its deviations is not based on ideal assumptions such as equipotential of sorption sites, absence of steric hindrances between sorbed and incoming particles and surface homogeneity on microscopic level [29]. The estimated constant, Q_D gives an idea about the mean free energy which was valued as less than one. E is a parameter used in predicting the type of adsorption. An E value < 8 $kJmol^{-1}$ is an indication of physisorption [30].

The DR Theoretical saturation capacity, Q_D and the Langmuir maximum adsorption capacity, Q_0 were both estimated as $Q_m = 105.62$ mgg^{-1} and $Q_D = 61.08$ mgg^{-1}. No known and proven reference could make us conclude that the theoretical saturation capacity, Q_D is always lesser than the maximum adsorption capacity as the case was made evidence in this research [31].

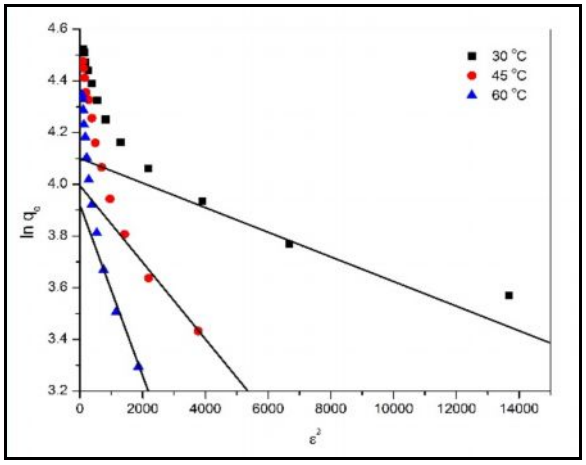

Fig. 6. Effect of DR plot for the adsorption of Acid Red 114 onto PWAC.

3.3.5. Halsey adsorption isotherm

The Halsey adsorption isotherm can be given as [32].

$$q_e = \exp\left[\frac{\ln K_H - \ln C_e}{n_H}\right]$$

and a linear form of the isotherm can be expressed as follows

$$\ln q_e = \frac{\ln K_H}{n_H} - \frac{\ln C_e}{n_H}$$

This equation is suitable for multilayer adsorption and the fitting of the experimental data to this equation attest to the heteroporous nature of adsorbent where K_H (mg/L) and n_H are the Halsay isotherm constants. The K_H and n_H values are represented in table 1. The plot $\ln q_e$ vs $\ln C_e$ was showed in Fig.7.

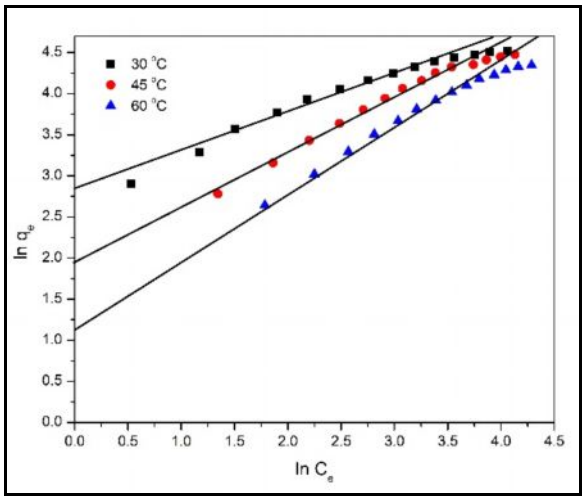

Fig. 7. Effect of Halsey isotherm plot for the adsorption of Acid Red 114 onto PWAC.

3.3.6. Jovanovic adsorption isotherm

The model of an adsorption surface considered by Jovanovic [33] is essentially the same as that considered by Langmuir. The Jovanovic model leads to the following relationship**.**

$$q_e = q_{max}(1 - e^{K_J C_e})$$

The linear form of the isotherm can be expressed as follows:

$$\ln q_e = \ln q_{max} - K_J C_e$$

Where K_J (L/g) is a parameter. K_J and q_{max} (mg/g) is the maximum acid red 114 uptake is represented in table 1 at different temperatures.

Table 2 List of different model isothermerror parameter values for acid red 114

Model	Isotherm Constants	Temperature		
		30 °C	**45 °C**	**60 °C**
Langmuir	SSE	0.0016	0.0023	0.0026
	χ^2	0.0192	0.0070	0.0040
	RMSE	0.0315	0.0444	0.0452
Freundlich	SSE	0.0331	0.0243	0.0172
	χ^2	0.0217	0.0156	0.0119
	RMSE	0.1748	0.1536	0.1243
Temkin	SSE	267.7789	391.9669	325.0601
	χ^2	17.4258	24.8387	23.6477
	RMSE	13.8772	17.6411	16.4450
Halsey	SSE	0.7098	0.2902	0.1664
	χ^2	0.1044	0.1360	0.0619
	RMSE	0.7992	0.5284	0.3860
D-R	SSE	2.1757	2.2181	2.1543
	χ^2	0.6264	0.6552	0.6655
	RMSE	1.4006	1.4461	1.4194
Jovanovic	SSE	0.0135	0.0163	0.0210
	χ^2	0.1215	0.1338	0.1520
	RMSE	930.6342	894.4267	850.1320

The SSE and chi square values for the Jovanovic model were slightly higher for Langmuir model. But RMSE value is higher than that of all other models indicate jovanovic did not suitable for the adsorption process. Fig.8 represents the jovanovic adsorption isotherm.

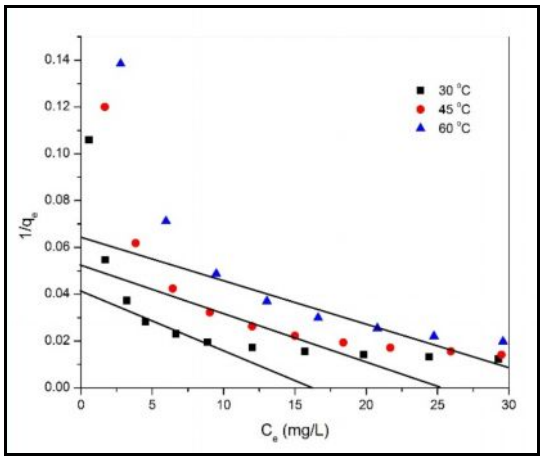

Fig. 8. Effect of Jovanovic isotherm plot for the adsorption of Acid Red 114 onto PWAC.

3.4. Error analysis

The error analysis values for Langmuir, Freundlich, Temkin, D-R, Halsey and Jovanovic isotherm models at 303, 313 and 333 K are presented in Table 2. it would seem (that), it can be concluded that the most applicable isotherm to relate Acid red 114-PWAC adsorption system is Langmuir isotherm. The values of regression coefficients, R^2 and the non-linear error functions (SSE, RMSE and chi-square) are in accordance to one another. despite the fact that the linear regression coefficients, R^2 of the Freundlich are less than 0.99 at 303,313 and 323 K. Thus, Langmuir is still considerable to describe this adsorption system. The D-R is the least applicable isotherm as the linear regression coefficients, R^2 were less than 0.7 and the non-linear error functions (SSE and chi-square) are higher in value at all temperature range. The SSE value more than 5% is not recommended due to intolerant margin of deviation between the experimental data and the model calculated data. The Halsey and Jovanovic isotherm regression coefficients, R^2 were less than 0.8 and the non-linear error functions (SSE and chi-square) are higher in value at all temperature indicates the non-suitability of adsorption. Langmuir models show a high degree of correlation with low root mean square error (RMSE), SSE and chi-square values.

3.5. Adsorption Kinetics

Kinetic models have been proposed to determine the mechanism of the adsorption process which provides useful data to improve the efficiency of the adsorption and feasibility of process scale-up [34]. Physical and chemical properties of the adsorbents as well as mass transfer processes are some influential parameters to determine the adsorption mechanism [35].The analysis of experimental data at various times makes it possible to calculate the kinetic parameters and to take some information for designing and modeling of the adsorption processes. To understand the adsorption mechanism of PWAC for acid red 114, the adsorption kinetics were investigated using pseudo first-order, pseudo-second order, Elovich and Intraparticle diffusion kinetic equation models.

3.5.1. Pseudo first-order kinetic model

The pseudo-first-order kinetic model [36] can be expressed as

$$\log(q_e - q_t) = \log q_e - \left(\frac{K_1}{2.303}\right)t$$

According to this equation, a plot of log (q_e-q_t) versus time should be linear. However, in our experiments, q_e remains unknown due to slow adsorption process and therefore, linearity in the plots of log(q_e-q_t) versus time (t) could not be observed. It has been observed in many cases that the first order equation of Lagergren does not fit well for the whole range of contact time and is generally applicable over the initial stage of adsorption process [37].

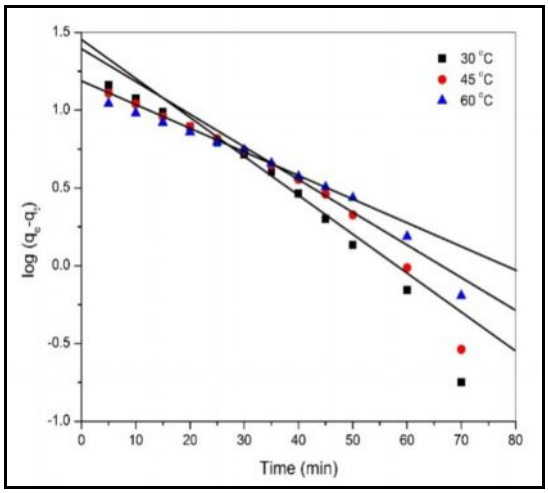

Fig. 9. Effect of Pseudo first order plot for the adsorption of Acid 114 onto PWAC

Fig. 9 shows a plot of linearization form of pseudo first-order model at different temperatures were studied. The slopes and intercepts of plots of $\log(q_e-q_t)$ versus t were used to determine the pseudo first-order constant k_1 and equilibrium adsorption density q_e. However, the experimental data deviated considerably from the theoretical data. A comparison of the results with the correlation coefficients is shown in Table 3. The correlation coefficients for the pseudo first order kinetic model obtained at all the studied temperatures were low. Also the theoretical q_e values found from the pseudo first-order kinetic model did not give reasonable values. These results suggest that the adsorption system is not suitable for pseudo first-order reaction [38].

3.5.2 Pseudo Second Order Kinetic Model

To describe the dye adsorption, the modified pseudo second order kinetic equation is expressed as [39]

$$\frac{t}{q_t} = \frac{t}{K_2 q_e^2} + \frac{1}{q_e} t$$

where K_2 is the rate constant of pseudo-second-order model (g/mg.min) and q_e is derived from the linear plot of t/q_t versus t. The second-order rate constant was used to calculate the initial adsorption rate (h) given by the equation

$$h = K_2 q_e^2$$

The rate constants and correlation coefficients (R^2) of the kinetic models are listed in table 1.

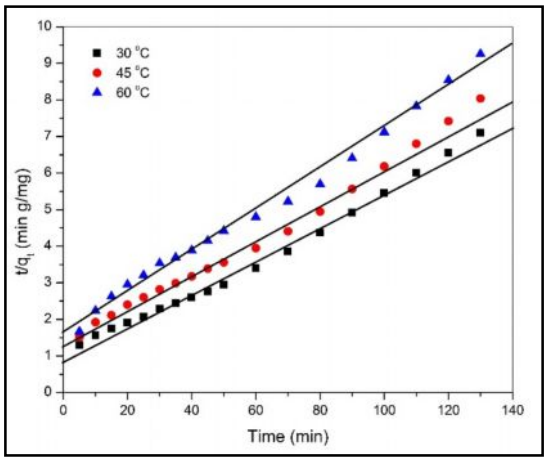

Fig. 10. Effect of Pseudo second order plot for the adsorption of Acid 114 onto PWAC

From the results, pseudo second-order kinetic model gave $R^2 > 0.99$ for all temperatures. The values of the rate constants decreased with increasing temperature. The q_e values calculated from the linear plot of the pseudo-second-order kinetic model were also found to be in agreement with experimental q_e values (table 3).

Since pseudo-second-order kinetic model fitted better with this system than the pseudo first-order kinetic model, coupled with the high agreement between its calculated and experimental q_e values it can be suggested that the adsorption was controlled by physisorption. This process involves valence forces through exchange of electrons between adsorbate and adsorbent. Also the decrease in rate constant K_2 as the temperature increases reveals the fact that it is faster for the adsorption system with acid red 114 to reach equilibrium.

3.5.3. Elovich model

We can write the Elovich kinetic model as [40]

$$\frac{dQ}{dt} = \alpha \exp(-\beta Q)$$

In this model, α is known initially as the rate of adsorption with the unit of $mg.g^{-1}.min^{-1}$. β is known as coefficient of desorption as $g.mg^{-1}$. We can rewrite the Elovich kinetic model equation, with assumptions of

αβt ≫ t and by using two boundary conditions. These conditions are Q = 0 for time of t = 0 and Q = Q_t for time of t = t. With these assumptions, the Elovich model equation can be written as

$$Q_t = \beta ln\alpha\beta + \frac{1}{\beta}\ln(t)$$

If acid red 114 adsorption with using PWAC obeys the Elovich kinetic model, Q_t vs lnt must give a line with a slope and intercept values of (1/β) and ln(αβ) respectively. This procedure has been applied in Fig. 11.

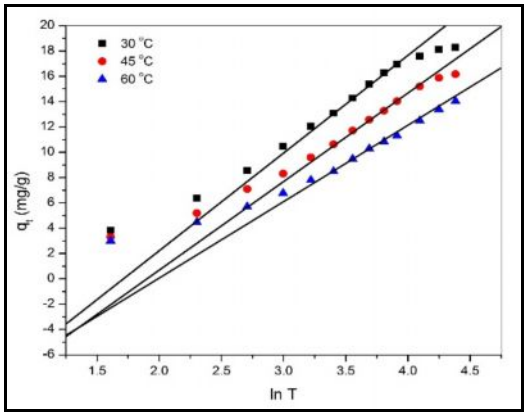

Fig. 11. Effect of Elovich plot for the adsorption of Acid 114 onto PWAC

The correlation coefficient R^2 showed that the pseudo-second-order model, indicative of a physisorption mechanism, fit the experimental data slightly better than the Elovich and the pseudo-first order models. In other words, the adsorption of acid red 114 could be approximated more favorably by the pseudo-second-order kinetic model.

Table 3 lists also the kinetic constants obtained from the Elovich equation. On increasing the temperature from 30 to 60 °C, the values of β have slight significant variation. However, the constant α increased as the temperature increased. This behavior suggests that more than one mechanism controls the adsorption process [41]. For the Elovich model, the correlation coefficients (R^2) are relatively high (>0.95). It indicates that the Elovich model can also be suitable for describing the adsorption kinetic of acid red 114 onto PWAC.

The Elovich equation provides the best correlation for all of the sorption process, whereas the pseudo second-order equation also fits the experimental data well. This suggests that the sorption systems studied belong to both the Elovich equation and the pseudo second-order kinetic model with experimental data. The adsorption system obeys the pseudo second-order kinetic model for the entire adsorption period and thus supports the assumption behind the model that the adsorption is due to physisorption.

3.5.4. Intraparticle Diffusion Model

The most-widely applied intraparticle diffusion equation for sorption which describes the diffusion mechanism and rate controlling steps given by Weber and Morris [42] is

$$q_t = k_{id} t^{1/2} + C$$

where, q_t is the fraction dye uptake (mg/g) at time t, k_{id} is the intra-particle diffusion rate constant (mg/g $min^{1/2}$) and C is the intercept (mg/g). The plot of q_t versus $t^{1/2}$ will give k_{id} as slope; C represents the effect of boundary layer thickness between solute and adsorbent. Minimum is the intercept length, adsorption is less boundary layer controlled.

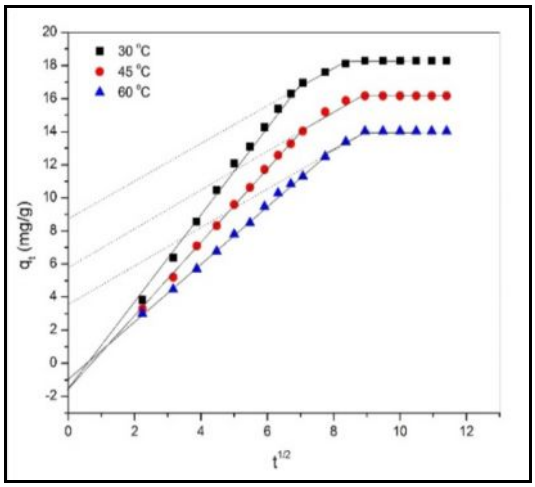

Fig. 12. Effect of Intraparticle plot for the adsorption of Acid 114 onto PWAC.

The correlation coefficient (R^2) values of intraparticle diffusion models were higher and also give the intercept value. The value of intercept indicates that the lines were not passing through origin, signifying that adsorption involved intraparticle diffusion, nevertheless that was not the only rate-controlling step [43], and thus some other adsorption process affect the intraparticle diffusion. This was due to the surface adsorption or boundary layer adsorption. Almost all the correlation coefficient (R^2) value was greater than 0.98 for 30 to 60 °C. So the intraparticle diffusion takes place along with the boundary layer effect [44].

Table 3 Kinetic parameters for the adsorption of Acid Red 114 onto PWAC

Kinetic Model	Kinetic Parameters	Temperature		
		30 °C	45 °C	60 °C
Pseudo-first Order	K_1 (min^{-1})	-0.0548	-0.0460	-0.0348
	R^2	0.9540	0.9308	0.9497
Pseudo-second Order	K_2 (g/mg min)	0.0023	0.0019	0.0018
	q_e	18.30	16.17	14.04
	h	1.1201	0.8064	0.6099
	R^2	0.9914	0.9902	0.9907
Elovich	α	2.2719	1.6683	1.3035
	β	0.2036	0.2206	0.2511
	R^2	0.9500	0.9668	0.9653
IPD	K_{id}	2.6199	2.2092	1.7563
	R^2	0.9880	0.9890	0.9988

3.5.5. Validity of kinetic model

Comparison of experimental and calculated value of equilibrium was found that the well-matched model to describe adsorption process. The applicability of these models were further validated by applying SSE, Chi square [45] and RMSE [46]. This approach allows a comparison of the scaled errors and thus identifies the parameter set that would provide the closest fit to the measured data.

$$SSE = \sum (q_{e,cal} - q_{e,exp})^2$$

$$RMSE = \sqrt{\frac{1}{N-2}\sum_{i=1}^{n}(q_{e,exp} - q_{e,cal})^2}$$

$$\chi^2 = \sum_{i=1}^{n}\frac{(q_{e,exp} - q_{e,cal})^2}{q_{e,exp}}$$

where, n is the number of data points. The values of SSE, RMSE and χ^2 for the pseudo first and pseudo second, Elovich kinetic models and Intraparticle diffusion models are given in table-4. It can be seemed that the SSE, RMSE and χ^2 value is lower for the second order kinetic model than that for the pseudo first order, Elovich and Intraparticle model. This conform a better applicability of the pseudo second order kinetic model. The correlation coefficient for the pseudo first order ranged between 0.93 and 0.95 whereas the values for the second order are closest to 1. The higher correlation coefficient and the lower the SSE, RMSE and χ^2 values confirm the better fitness of the model. The correlation coefficient indicates that the experimental data best fitted into the pseudo second order, then the process of adsorption follows Elovich kinetic model of its chi square and regression values. This lowest value of error analysis parameter confirms pseudo–second order Type II and Type IV followed by Elovich model as best fit model to describe the adsorption process of Acid red 114-PWAC system.

Table 4 Kinetic Error parameters for the adsorption of Acid Red 114 onto PWAC

Kinetic Model	Error Parameters	Temperature		
		30 °C	45 °C	60 °C
Pseudo-first Order	SSE	2.4709	3.1004	3.4429
	χ^2	1.5601	16.5150	2.2930
	RMSE	1.5203	1.7110	1.8364
Pseudo-second Order	SSE	0.4827	0.5775	0.7719
	χ^2	0.1696	0.1392	0.1736
	RMSE	0.7444	0.7816	0.8810
Elovich	SSE	17.8860	9.9414	6.7268
	χ^2	1.2359	0.8445	0.8965
	RMSE	4.4184	3.4215	2.7196
IPD	SSE	58.7992	33.2548	16.5443
	χ^2	6.3893	3.7325	1.8427
	RMSE	8.1795	6.1821	4.2730

3.6. Adsorption Thermodynamics

The standard Gibbs free energy ΔG^o(kJ mol^{-1}), standard enthalpy change ΔH^o (kJ mol^{-1}), and standard entropy change ΔS^o (J $mol^{-1}K^{-1}$) were calculated using the following equations:

$$\Delta G^0 = -RT\ln K_0$$

$$\ln K_0 = \frac{\Delta S^0}{R} - \frac{\Delta H^0}{RT}$$

Where R is the universal gas constant (8.314 J mol^{-1} K^{-1}), T is the temperature in Kelvin and K_0 is the equilibrium constant.

The plot of ln K_0 vs. 1/T was linear and the values of ΔH^0 and ΔS^0 were resolved from the slope and intercept. The values of these parameters are show in table 5. The value of enthalpy change ΔH^0 (-42.55 $KJmol^{-1}$) is negative indicating the adsorption is exothermic process.

Table 5 Thermodynamic parameters for the adsorption of Acid red 114 onto PWAC

Dye	T(K)	ΔG^0 (kJ/mol)	ΔH^0 (kJ/mol)	ΔS^0(kJ/mol K)
AR 114	303	-5.9827	-42.554	-121.06
	318	-3.8081		
	333	-2.3739		

The negative values of ΔG° at all temperatures (30, 45 and 60 °C, respectively) verified the thermodynamic feasibility and spontaneity of the adsorption process. The negative value of ΔS° (-121.06 J. $mol^{-1}K^{-1}$) suggests that the disorder at the solid−liquid interface decreased during dye adsorption and that no significant changes occurred in the internal structure of the adsorbents upon adsorption [47]. When the value of ΔS^0 is higher than -10 kJ mol^{-1}, a dissociative mechanism controls the adsorption process [48-50]. The values of ΔG^0 at all temperatures studies as presented in table 2 were indications that the sorption process was physisorption since the values are between-20 to 0 kJ mol^{-1} [51].

Conclusions

In this present study, plastic wastes were converted to activated carbon as low cost sorbent for the sorption of dyes from textile industrial effluents. SEM and XRD showed that the adsorbent material has a micro porous and crystalline structure. Equilibrium data fitted very well in the Langmuir isotherm equation, confirming the monolayer adsorption capacity of acid red 114 onto PWAC with a monolayer adsorption capacity of 135.79 mg/g. The linear analysis shows the adsorption process was strongly followed Langmuir adsorption isotherm model.

The rate of adsorption is decrease with increase in temperatures. The kinetic of adsorption of acid red 114 obeyed well with the pseudo-second-order model. The results of the intraparticle diffusion model suggest that the diffusion was not found the rate determining step. Thermodynamic study reveals the spontaneous and exothermic nature of adsorption process owing to negative values of free energy and enthalpy change. The adsorption technique is favourable for the physisorption mechanism. The validity of the kinetic models analyzed using SSE, Chi square and RMSE methods find the adsorption is best opted by pseudo second order kinetic model.

Acknowledgement

The authors say a grateful thanks to Dr.Sabde, Sud-Chemie India Pvt. Ltd for providing the catalyst in this research.

References

1. Richard C. Thompson, Charles J. Moore, Frederick S. vomSaal, Shanna H. Swan. Plastics, the environment and human health: current consensus and future trends, Phil. Trans. R. Soc. B 364 (2009) 2153.
2. H. Yasuda, O. Yamada, A. Zhang, K. Nakano, M. Kaiho, Hydrogasification of coal and polyethylene mixture. Fuel. 83 (2004) 2251.
3. P.V.Thorat, SandhyaWarulkar, HarshalSathone, Thermofuel-Pyrolysis of waste plastic to produce Liquid Hydroocarbons, Advan. Polym. Sci. Technol. 3 (2013) 14.
4. Chika Muhammad, Jude A. Onwudili, and Paul T. Williams, Thermal Degradation of Real-World Waste Plastics and Simulated Mixed Plastics in a Two-Stage Pyrolysis−Catalysis Reactor for Fuel Production, Energy Fuels in press.

5. Christina Dorado, Charles A. Mullen, and Akwasi A. Boateng, H-ZSM5 Catalyzed Co-Pyrolysis of Biomass and Plastics, | ACS Sustainable Chem. Eng. 2 (2014) 301−311.
6. D. P. Serrano, J. Aguado, and J. M. Escola, Developing Advanced Catalysts for the Conversion of Polyolefinic Waste Plastics into Fuels and Chemicals, ACS Catal., 2 (2012) 1924−1941.
7. A. Marcilla, M.I. Beltrán, Beltrán, Navarro, Thermal and catalytic pyrolysis of polyethylene over HZSM5 and HUSY zeolites in a batch reactor under dynamic conditions, Appl. Catal. B. Environ. 86 (2009) 78.
8. Y.H. Lin, M.H. Yang, Catalytic reactions of post-consumer polymer waste over fluidised cracking catalysts for producing hydrocarbons, J. Mol. Catal. A: Chem. 231 (2005) 113.
9. J.F. González, S. Román, J.M. Encinar, G. Martínez, Pyrolysis of various biomass residues and char utilization for the production of activated carbons, J. Anal. Appl. Pyrol. 85 (2009) 134.
10. A.H. Jalil, Surface area determination of activated carbons produced from waste tires using adsorption from solution, Tikrit J. Pure Sci. 17 (2012).
11. E.L.K. Mui, W.H. Cheung, M. Valix, G. McKay, Dye adsorption onto activated carbons from tyre rubber waste using surface coverage analysis, J. Colloid Interface Sci. 347 (2010) 290.
12. F. Lian, Z. Song, Z. Liu, L. Zhu, B. Xing, Mechanistic understanding of tetracycline sorption on waste tire powder and its chars as affected by Cu^{2+} and pH, Environ. Pollut. 178 (2013) 264.
13. H. Guedidi, L. Reinert, Y. Soneda, N. Bellakhal, L. Duclaux. Adsorption of ibuprofen from aqueous solution on chemically surface-modified activated carbon cloths, Arab. J. Chem. (2014) In press.
14. A.R. Binupriya, M. Sathishkumar, S.H. Jung, S.H. Song, S.I. Yun, A novel method in utilization of Bokbunja seed wastes from wineries in liquid-phase sequestration of Reactive Blue 4, Int. J. Environ. Res. 3 (2009) 1-12.
15. P. Balakrishna Murthy, A. Sairam Kishore, P. Surekha, Acute toxicological effects of multi-walled carbon nanotubes (MWCNT). Nanotechnology and Nanomaterials-Carbon Nanotubes - Growth and Applications, book edited by Dr. Mohammad Naraghi, ISBN 978-953-307 (2008).
16. S. Lu, D. Cao, X. Xu, H. Wang, Y. Xiang, Study of carbon black supported amorphous Ni–B nano-catalyst for hydrazine electro-oxidation in alkaline media, RSC Adv. 4 (2014) 26940–26945.
17. B.R. Venkatraman. U. Gayathri, S. Elavarasi, S. Arivoli, Removal of Rhodamine B dye from aqueous solution using the acid activated Cynodondactylon carbon, Der. Chemica. Sinica, 3 (2012) 99-113.
18. Z. Xie, W. Guan, F. Ji, Z. Song, Y. Zhao, Production of biologically activated carbon from orange peel and landfill leachate subsequent treatment technology, J. Chem. (2014) 1-9.
19. M. F. Elkady, M. M. Hussein, M. M. Salama, Synthesis and characterization of nano-activated carbon from el maghara coal, Sinai, Egypt to be utilized for wastewater Purification, Am. J. Appl. Chem. 3 (2015) 1-7.
20. W. Zhang, D. Yu, X. Jia, H. Huang. Efficient dehydration of bio-based 2,3-butanediol to butanone over boric acid modified HZSM-5 zeolites. Green Chem., 14 (2012) 3441.
21. A. Khaled, A. El Nemr, A. El-Sikaily, O. Abdelwahab, Treatment of artificial textile dye effluent containing Direct Yellow 12 by orange peel carbon, Desalination. 238 (2009) 210-232.
22. I. Langmuir, The constitution and fundamental properties of solids and liquids, J. Am. Chem. Soc. 38 (1916) 2221–2295.
23. B. Abbad, A. Lounis, K. Taibi, M. Azzaz, Removal of methylene blue from coloured effluents by adsorption onto ZnAPSO-34 nanoporous material, J. Mater. Sci. Eng. 2 (2013) 1-6.
24. H.M.F. Freundlich, Over the adsorption in solution, J. Phys. Chem. 57 (1906) 385–471.
25. P.S. Syed Shabudeen, Adopting response surface methodology to design an experiment in studying the removeal of dye by utilizing solid agricultural waste activated carbon, Int. J. Sci. Technol. 1 (2011) 118-127.
26. M.I. Tempkin, V. Pyzhev, Kinetics of ammonia synthesis on promoted iron catalyst, Acta Phys. Chim. USSR. 12 (1940) 327–356.
27. M.M. Dubinin, E.D. Zaverina, L.V. Radushkevich, Sorption and structure of active carbons, I. Adsorption of organic vapors. ZhurnalFizicheskoiKhimii. 21 (1947) 1351–1362.
28. W. Rieman, H. Walton, Ion Exchange in Analytical Chemistry, International Series of Monographs in Analytical Chemistry, Pergamon Press, Oxford, 1970.
29. J. Monika, V. Garg, K. Kadirvelu, Chromium (VI) removal from aqueous solution, using sunflower stem waste, J. Hazard. Mater. 162 (2009) 365–372.

30. A.U. Itodo, H.U.Itodo, Utilizing D-R and Temkin isotherms with GCMS external standard technique in forecasting liquid phase herbicide sorption energies. Electronic J. Environ. Agri. Food Chem. 9 (2010) 1792-1802.
31. E. Malkoc, Y. Nuhoglu, Determination of kinetic and equilibrium parameters of the batch adsorption of Cr(VI) onto waste acorn of Quercusithaburensis, Chem. Eng. Process. 46, (2007), 1020-1029.
32. Y.S. Ho, J.F. Porter, G. Mckay, Equilibrium isotherms studies for the sorption of divalent metal ions onto peat: copper, nickel and lead single component systems, Water, Air and Soil Pollut. 141 (2002) 1-33.
33. M. Jaroniec, Adsorption of gas mixtures on homogeneous surfaces Extension of Jovanovic equation on adsorption from gaseous mixtures, Chem. Zvesti. 29 (1975)512.
34. M. F. Elkady, M. M. Hussein, M. M. Salama, Synthesis and characterization of nano-activated carbon from el maghara coal, Sinai, Egypt to be utilized for wastewater Purification, Am. J. Appl. Chem. 3 (2015) 1-7.
35. M. Mohammadi, A.J. Hassani, A.R. Mohamed, G.D. Najafpour. Removal of Rhodamine B from aqueous solution using palm shell-based activated carbon: adsorption and kinetic studies, J. Chem. Eng. Data. 55 (2010) 5777–5785.
36. S. Lagergren. About the theory of so-called adsorption of soluble substances, Kungliga Sven. Vetensk. Handl. 24 (1898) 1–39.
37. S. Chandravanshi, S.K. Upadhyay, Kinetic, equilibrium and thermodynamic studies of adsorption of terminaliaarjuna natural dye on cotton in presence of cationic surfactant, Int. J. Fiber. Text. Res. 4 (2014) 20-26.
38. M. Al-Meshragi, H.G. Ibrahim, M.M. Aboabboud, Equilibrium and kinetics of chromium adsorption on cement kiln dust. Proc. World Congress Eng. Computer Sci., San Francisco, USA, 2008.
39. D. Sun, X. Zhang, Y. Wu, X. Liu, Adsorption of anionic dyes from aqueous solution on fly ash, J. Hazard. Mater. 181 (2010) 335–342.
40. H.Qiu, L. LV, B. Pan, Q. Zhang, W. Zhang, Q. Zhang, Critical review in adsorption kinetic models, J. Zhejiang Univ. Sci. A. 10 (2009) 716-724.
41. M.A. Ahmad, N.A.A. Puad, O.S. Bello. Kinetic, equilibrium and thermodynamic studies of synthetic dye removal using pomegranate peel activated carbon prepared by microwave-induced KOH activation, Water Resour. Ind. 6 (2014) 18–35.
42. W.J. Weber Jr., J.C. Morris, Kinetics of adsorption on carbon from solution, J. Sanit. Eng. Div. ASCE. 89 (1963) 31–59.
43. H. El-Boujaady, M. Mourabet, M. Bennani-Ziatni, A. Taitai, Adsorption/desorption of Direct Yellow 28 on apatitic phosphate: Mechanism, kinetic and thermodynamic studies, J. Asso. Arab Uni. Basic Appl. Sci. 16 (2014) 64–73.
44. M. Thilagavathi, S. Arivoli, V. Vijayakumaran. Kinetic and thermodynamic studies on the adsorption behavior of RhodamineB dye using ProsopisJuliflora bark carbon, Sci. J. Eng. Tech. 2 (2014) 258-263.
45. H. Guedidi, L. Reinert, Y. Soneda, N. Bellakhal, L. Duclaux. Adsorption of ibuprofen from aqueous solution on chemically surface-modified activated carbon cloths, Arab. J. Chem. 2014 in press.
46. M.A. Hossain, H.H. Ngo, W.S. Guo and T.V. Nguyen. Biosorption of Cu(II) from water by banana peel based biosorbent: experiments and models of adsorption and desorption, J. Water Sustainabil. 2 (2012) 87–104.
47. A. Roy, B. Adhikari, S.B. Majumder, Equilibrium, Kinetic, and Thermodynamic studies of azo dye adsorption from aqueous solution by chemically modified lignocellulosic jute fiber. Ind. Eng. Chem. Res. 52 (2013) 6502−6512.
48. B.W. Hu, W. Cheng, H. Zhang, S.T. Yang, Solution chemistry effects on sorption behavior of radionuclide 63Ni(II) in illite-water suspensions, J. Nucl. Mater. 406 (2010) 263–270.
49. S. Yang, D. Zhao, H. Zhang, S. Lu, L. Chen, X. Yu. Impact of environmental conditions on the sorption behavior of Pb(II) in Na-bentonite suspensions, J. Hazard. Mater. 183 (2010) 632–640.
50. S. Yang, Z. Guo, G. Sheng, X. Wang, Investigation of the sequestration mechanisms of Cd(II) and 1-naphthol on discharged multi-walled carbon nanotubes in aqueous environment, Sci. Total. Environ. 420 (2012) 214–221.
51. O. Alao, J.A. Chijioke, O. Ayeni, Kinetics, equilibrium and thermodynamic studies of the adsorption of Zinc(II) ions on Carica papaya root powder, Res. J. Chem. Sci. 4 (2014) 32-38

*****